A new explicit dynamic path tracking controller using Generalized Predictive Control

Mohamed Krid, Faiz Benamar, and Roland Lenain

Abstract: Outdoor mobile robots has to perform operations more and more far and more and more quickly. Therefore we are interested in design controller of fast rovers which make able autonomous mobile robot to move in natural environment at high velocity and following a reference path. Taking into consideration the wheel slippage is of primary importance in this kind of conditions. The paper presents a path tracking controller for a fast rover which has independent front and rear steering. In the first step, the dynamic model of the vehicle moves on a horizontal plane was developed. Next, the projection of the position of the vehicle in the absolute reference frame is used to define the kinematics non-linear model. We present a new approach to solve a tracking path problem by applying Non-linear Continuous-time Generalized Predictive Control (NCGPC). The controller is based on the dynamic model of a bicycle like vehicle which considers the lateral slippage of wheels. The prediction model allows to anticipate future changes in setpoints in accordance with the dynamic constraints of the system. Experimental results, show a good control accuracy and appears to be robust with respect to environment and robot state changes.

Keywords: Mobile robot, Path tracking, Nonlinear Continuous-time Generalized Predictive Control, Modeling.

1. INTRODUCTION

The motion control of an unmanned Ground Vehicle (UGV) is often defined through a path or trajectory tracking problem. The reference path is in general given by the high level controller i.e. the planner and could be updated continuously as function of actual environment conditions. Classically, this problem is addressed using kinematic models in a Frénet frame (i.e attached to the path to be followed, see [1]). Such kind of models are moreover popular because of the simplicity of their structure [2] and their properties of exact linearizability. Such models are based on the popular Rolling Without Sliding (RWS) assumption, offering good performances in on-road applications, and/or moving with limited speed (such as shown in [3], or in [4]). Nevertheless, as it can be expected and well pointed out in [5] or [6], the motion in natural environment using the RWS assumption is no more relevant. Accuracy in this kind of solution indeed decreases in a remarkable way when the vehicle dynamics and the sliding become important mostly for high speed robots. This may penalize the robotic task execution when considering off road applications such as defense, exploration or agriculture.

To face the uncertainty of the model and the ground perturbations, several approach may be investigated. First, sliding effects may be viewed as a perturbation of classical kinematic model [7], to be rejected by robust control strategy [8]. Such point of view nevertheless appears to be conservative, since an error has first to occur before being compensated. A second approach, allowing to preserve a kinematic description, lies in the consideration of an extended kinematic model [9], [10]. Side-slip angles, defined as the difference between tire orientation and actual speed vector direction permits to account for influence of sliding into motion. These alternative models has to rely on adaptive approach in order to indirectly estimate the side-slip angles in real time. Such a control strategy obtain satisfactory results whatever the grip conditions, but the accuracy remains unsatisfactory at high speed, since dynamic phenomena are neglected. At important speed, dynamical effects are indeed no more negligible as well as actuator settling times or sensor delays. As a result, dynamical models have to be considered and predictive approaches to be favored [10]. For instance, in [11], a predictive and

This work was supported by the
(e-mail: med.krid@gmail.com).
Mohamed Krid, Faiz Benamar, ISIR - Institut des Systèmes Intelligents et Robotiques, Universite Pierre et Marie Curie Paris 6, CNRS UMR 7222 PARIS, 75252 cedex 05, France. (e-mail: amar@isir.upmc.fr).
Roland Lenain, Irstea - Institut national de Recherche en Sciences et Technologies pour l'Environnement et l'Agriculture, 63178 Aubière cedex, France (e-mail: roland.lenain@irstea.fr).

adaptive control law is developed to achieve off-road, path tracking at high speed working with several kind of motion model (extended kinematic and dynamic). Unfortunately, both kinematic and dynamic model remains non-linear and the above mentioned approach only consider classical Model Predictive Control algorithm, requiring a partial inexact linearization.

In this paper, a Nonlinear Continuous-time Generalized Predictive Control (NCGPC) approach is proposed, and based only on a dynamic representation of a car like mobile robot. Contrarily to other point of views, a linearization is not necessary, and dynamical effects are naturally considered by the model. In order to anticipate for transitions phases and compensate for consequent overshoots, the future path is considered, as well as the estimated future state. This control strategy appeared in 1962 with Zadeh and Wahlen works [12]. It was recognized in the world industry by [13] in the petrochemical field which is known by the process dynamic length. Later the approach was adopted to rapid systems [14] and [15] and mobile robotics [16] [17]. This control technique is used to ensure the path following task. In this case, the path prediction is achieved by taking into account the future changes during a constant horizon of prediction. Once the future position and path properties are estimated, a new control law for front steering angle is computed, the performance of which are considered to be independent from the robot longitudinal velocity.

This paper is organized as follow. Section 2 first begins with a description of the vehicle dynamic model with 3 Degrees Of Freedom (DOF) and using a linear slippage model. A second step proposes the reformulation of the model with respect to the path tracking tasks. Using this model a on linear predictive control is computed, dedicated to achieve an accurate path tracking despite the dynamical phenomena and the bad grip conditions. After having brought the proof of stability, the performances of the control law are investigated through full scale experiments using an electrical car like mobile robot.

2. WHEELED MOBILE ROBOT MODEL

2.1. Lateral dynamic model in robot frame

In this paper, the path tracking of a car like mobile robot with four steering wheels is considered in a slippery surface and at relatively high speed. As a result, ideal grip conditions cannot be assumed and dynamical effects have to be taken into account. A dynamical model of vehicle should then have to be considered (see [18] for a collection of several approaches). Since the motion on the ground with respect to a known trajectory is here considered, complete three dimensional models are useless, and only a two dimensional model is here considered. As depicted on the figure 1, the robot is viewed from top and only the motion is assumed to be achieved on flat horizontal plane. A complete model requires the knowledge of numerous parameters, and in this case, the vehicle horizontal plane motion is here mainly investigated. Moreover, the mobile robot is supposed to be symmetric with respect to a vertical plane containing middle of rear and front axle, also containing the center of mass G. As a result, the robot is viewed as a bicycle, one wheel describing the front axle, and a second one dedicated for the rear axle. The robot motion can then be described with respect to the moving point G, using the following notations, used all along the following of the paper:

- $R(X,Y,Z)$: The frame attached to the ground
- $R_1(x_1,y_1,z_1)$: The frame attached to the vehicle
- ψ: The vehicle yaw angle
- β_f,β_r: The front and rear steering angles
- α_f,α_r: The front and rear side-slip angle
- V_x,V_y: The longitudinal and lateral velocities of the chassis center of mass
- a,b: The front and rear vehicle half-wheelbases
- M: The vehicle mass
- I_z: The yaw-inertia moment
- $F_{x_{(f,r)}},F_{y_{(f,r)}}$: The longitudinal and lateral tire forces

Using these notations, the dynamical model of the robot motion in the horizontal plane may be derived. Since only the lateral motion control with respect to the path to be followed is addressed, the longitudinal forces are neglected $F_{x_{(f,r)}}=0$ and the longitudinal velocity V_x is supposed to be slow varying $\dot{V}_x=0$, and measured. This assumption is not really restrictive. The forthcoming lateral control (using front and rear steering angles β_f,β_r), will indeed be computed to have performances independent from the measured velocity.

The key point when computing a dynamic model for the vehicle motion lies in the expression of contact forces. In this approach the point is then to derive an expression for $F_{y_{(f,r)}}$, allowing to compute the motion equations. Various models were developed in order to study the tire ground contact behavior and determine analytical equations. One can first cite the contact models such as LuGre or Dahl model (defined for instance in [19] or [20]), based on the dynamic friction model. They are mainly representative of solid friction, neglecting the elasticity of tire, and are often not representative enough of the actual behavior, especially in off-road conditions. Another important approach is an empiric approach that conducted to "magic" formula such as the celebrated Pacejka formula [21] that express analytically the contact forces

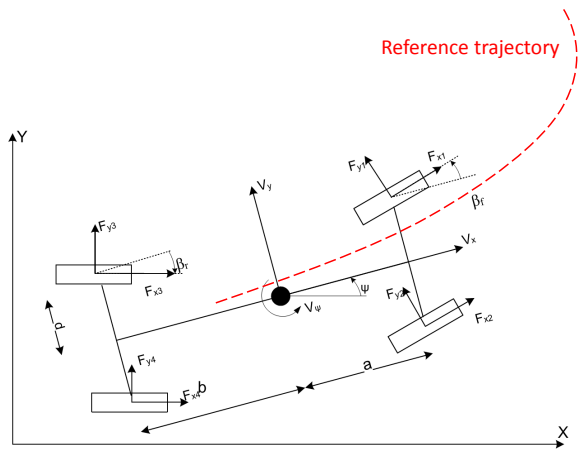

Fig 1: Model of the four-wheeled mobile robot, with dynamics parameters.

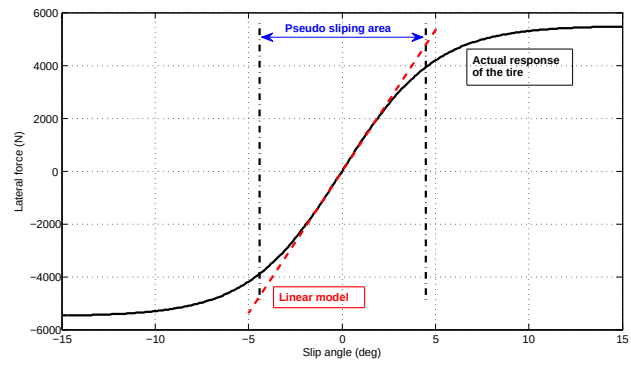

Fig 2: Nonlinear tire behavior, reduced to a pseudo sliping area.

with respect to the apparent side-slip angles. Such a relationship is deduced from experimental tests, and is parametrized by 12 parameters for the lateral effort and 8 parameters for the longitudinal effort. The figure 2 illustrate the contact behavior through an example of a Pacejka model. The shape depends on the wheel vertical load, while the parameters to be identified relies on the kind of tire, the pressure, the ground properties. All this properties are difficult to obtain and appears to be variable when moving off road at important speed.

Nevertheless, contact models shows that the relationship between forces and side-slip angles may be approximated as a linear function when side-slip angles are considered to be small. This hypothesis is for instance admitted in [22] in order to estimate for the roll dynamics, or for the yaw dynamics in [23]. The expression of lateral forces whatever need the knowledge of side-slip angles, which is hardly achievable by a direct measure. In order to overcome such a difficulty, the researchers were brought to develop observers and indirect estimation for these variables, based on GPS and/or inertial measures (see [24] [25]). The estimation of side-slip angles together with the considered linear form of the lateral contact forces as expressed by (1), then permits to simplify the motion equations for the mobile robot.

$$F_{y_{(f,r)}} = C_{(f,r)}\alpha_{(f,r)} \tag{1}$$

C_f and C_r are, respectively, the tire cornering stiffness of the front and rear tires. These two parameters are estimated off-line and are assumed to be constant. Nevertheless, it considerably varies depending on the type of the ground, and vertical load, and the assumption of constant and known grip conditions is here supposed to be counterbalanced by the robustness of the approach. This permits to obtain a constant dynamic matrix and to test a new controller and its robustness with respect to parameters uncertainty. The side-slip angle $\alpha_{f,r}$ is defined as the angle between the wheel velocity and the longitudinal axis of the wheel itself. Assuming that side-slip angles are quite small (less than 10° in practice), we can use a linear model approximation of side-slip angle on the pseudo sliping area presented in figure 2, that is:

$$\alpha_f = \frac{V_y + a\dot{\psi}}{V_x} - \beta_f, \alpha_r = \frac{V_y - b\dot{\psi}}{V_x} - \beta_r \tag{2}$$

As it has been pointed out, the paper is focused on the lateral motion control (path tracking), on an horizontal plane. As a result, In this paper, we focus on the lateral dynamic and path tracking. As a result, the longitudinal velocity V_x will be considered constant ($\dot{V}_x = 0$), while longitudinal forces, together with the gravity are considered to have no influence on the robot motion. One can consequently derive the dynamical model from fundamentals of dynamics, leading to model (3), using linear contact forces (see [18] for more details)

$$\begin{pmatrix} \dot{V}_y \\ \ddot{\psi} \end{pmatrix} = A \begin{pmatrix} V_y \\ \dot{\psi} \end{pmatrix} + B \begin{pmatrix} \beta_f \\ \beta_r \end{pmatrix} \tag{3}$$

where A and B are 2×2 matrix of:

$$A = \begin{bmatrix} a_{11} & a_2 \\ a_{21} & a_{22} \end{bmatrix} = \begin{bmatrix} 2\frac{C_f + C_r}{M\ V_x} & 2\frac{a\ C_f - b\ C_r}{MV_x} - V_x \\ 2\frac{a\ C_f - b\ C_r}{V_x I_z} & 2\frac{a^2 C_f + b^2 C_r}{V_x I_z} \end{bmatrix}$$

and

$$B = \begin{bmatrix} b_{11} & b_2 \\ b_{21} & b_{22} \end{bmatrix} = \begin{bmatrix} \frac{-2\ C_f}{M} & \frac{-2\ C_r}{M} \\ \frac{-2\ a\ C_f}{I_z} & \frac{2\ b\ C_r}{I_z} \end{bmatrix}$$

This model is here defined in a frame attached to the robot, giving the evolution of lateral velocity $\dot{V}_y$ and yaw rate (angular velocity $\dot{\psi}$). Such equations may permit to act on a vehicle dynamics (such as ESP) in parallel of a manual driving, but does not permit to achieve autonomous control. In order to go further and achieve autonomous path tracking, the motion equations with respect to a desired trajectory (expressing successive positions in an absolute frame) has now to be computed from (3).

2.2. Modeling for path tracking control

The previous model (3) expresses the accelerations in a frame attached to the robot. In this paper, trajectory tracking is considered, and the derivative of the position as to be derived. As a result, the state space is enhanced with the orientation ψ and the robot absolute position (X,Y) of the robot in an absolute frame R. The trajectory to be followed is defined as a collection of successive coordinates expressed in the same absolute frame. Considering the kinematic description of the motion and the dynamic equations, one can derive the following motion model, defining the derivative of the robot position and orientation.

$$\begin{array}{l} \dot{V}_x = 0 \\ \dot{V}_y = a_{11}V_y + a_{12}V_\psi + b_{11}\beta_f + b_{12}\beta_r \\ \dot{V}_\psi = a_{21}V_y + a_{22}V_\psi + b_{21}\beta_f + b_{22}\beta_r \\ \dot{\psi} = V_\psi \\ \dot{X} = V_x \cos\psi - V_y \sin\psi \\ \dot{Y} = V_x \sin\psi + V_y \cos\psi \end{array} \tag{4}$$

The output y to be controlled is defined by:

$$y = \begin{pmatrix} \psi \\ X \\ Y \end{pmatrix}$$

while the control vector is composed of front and rear steering axles, since V_x is supposed to be uncontrolled in this paper:

$$u = \begin{pmatrix} \beta_f \\ \beta_r \end{pmatrix}$$

The bad grip conditions together with the actuator settling times generates delays and perturbations depreciating the accuracy of tracking task, see [9] for some highlighting experiments, and the result section. This is especially the case at the high speed context investigated in this paper. If bad grip conditions in steady state may be considered thanks to dynamic modeling, the delay during transient phases in mobile robot behavior have to be anticipated. Since the desired trajectory is entirely known by definition, a predictive control scheme may be applied. Nevertheless, the model (4) is non linear. A linear kinematic model is often used [26] to simplify the controller form. In our case, a non linear kinematic model is preserved in order to improve the model relevancy. As a result, a Non-linear Continuous-time Generalized Predictive Control (NCGPC) is used in this paper and is developed in the next sections. Optimal control problems are generally non-linear and therefore, it generally does not have analytic solutions like the linear-quadratic optimal control problem. The NCGPC controller present a solution for a both problems and simple to integrate in the robot calculator.

3. DESIGN NCGPC CONTROLLER

3.1. Multi-input multi-output non linear system

Predictive control is based on the minimization of a quadratic cost function that is compounded by the error between the predicted output and the reference. The advantage of this method is that it can be applied to the non-linear systems in the state, whence the name "Non-linear Continuous-time Generalized Predictive Control" (NCGPC). The prediction is based on a Taylor series expansion and knowledge derived from the dynamic function of the system until the said order relative degree. In this section we present this technique applied to multi-multi-output systems (MIMO). Obviously, the method can be applied to systems of single-input single-output (SISO), it is sufficient for it to reduce the size of the input and output one. This technique was developed in [27] for a system whose output number is equal to the number of entries. We generalize here for any system.

To introduce the design of NCGPC controller, we can write the dynamic model (4) in the following form:

$$\begin{array}{l} \dot{x} = f(x) + \sum_{i=1}^{p} g_i(x)u_i \\ y = \begin{pmatrix} h_1(x), & \ldots, & h_m(x) \end{pmatrix} \end{array} \tag{5}$$

where, the state vector $x \in X \subset \Re^n$, the output $y \in Y \subset \Re^m$ and input $u_i \in U \subset \Re^p$. The NCGPC controller minimizes a quadratic cost criterion which is based on the difference between the predicted state y and a reference signal w. We denote $e_i(t)$ the error between the output h_i and the reference signal $w_i(t)$ at the time t and $w = \begin{pmatrix} w_1(t) & \ldots & w_m(t) \end{pmatrix}$.

$$e_i(t) = h_i(x(t)) - w_i(t) \tag{6}$$

We can define the cost function as following

$$J_i = \frac{1}{2}\int_0^{T_i} [\hat{e}_i(t+\tau)]^2 d\tau \tag{7}$$

where T_i is the prediction horizon time of the ith output h_i and τ a given instant belonging to interval $[t, t+T_i]$. We deduce the global cost function J:

$$J = \sum_{i=1}^{m} J_i = \frac{1}{2}\sum_{i=1}^{m}\left(\int_0^{T_i}[\hat{e}_i(t+\tau)]^2 d\tau\right) \tag{8}$$

To derive the control law, we need to minimize the expression (8) of the criterion with respect to control u:

$$\frac{\partial J}{\partial u} = 0_{p\times 1} \tag{9}$$

Before defining the predicted error, we need to introduce the Lie derivatives of non-linear function. Then, we predict the output of our system and with the reference trajectory we define the error prediction. Finally we deduce the expression criterion and the control law.

3.2. Lie derivatives

In this paper the standard geometric notation for Lie derivatives is used. The Lie derivative of a output function h_i along f in $x \in \Re^n$, is giving by:

$$L_f h_i(x) = \sum_{j=1}^{n} \frac{\partial h_i}{\partial x_j}(x) f_i(x) \tag{10}$$

with $1 \le j \le p$ and $1 \le i \le m$ Inductively, we define

$$L_f^k h_i(x) = L_f L_f^{k-1} h_i(x) = \frac{\partial L_f^{k-1} h}{\partial x}(x) f(x) \tag{11}$$

with $L_f^0 h_i(x) = h_i(x)$.

We define ρ a vector of relative degrees of a non-linear MIMO system. It is composed by the different values of relative degree ρ_i of each output h_i. The relative degree of output is the minimum number of derivative required to make explicit in it's expression one component of the input vector.

A non-linear MIMO system, of the form (5), has a relative degree vector $\rho = \begin{pmatrix} \rho_1(t) & \dots & \rho_m(t) \end{pmatrix}$ around x^0 if:

1. $L_{g_j} L_f^k h_i(x)) = 0$ for all $1 \le j \le p$, for all $k \prec \rho_i - 1$, for all $1 \le i \le m$ and for all x in a neighborhood of x^0
2. the matrix $D(x)$ of ~~dimension$m \times m$~~ dimension$m \times p$, called decoupling matrix, given by:

$$D(x) = \begin{bmatrix} L_{g_1} L_f^{\rho_1 - 1} h_1(x) & \dots & L_{g_p} L_f^{\rho_1 - 1} h_1(x) \\ \vdots & \ddots & \vdots \\ L_{g_1} L_f^{\rho_m - 1} h_m(x) & \dots & L_{g_p} L_f^{\rho_m - 1} h_m(x) \end{bmatrix} \tag{12}$$

is non-singular matrix in $x = x^0$.

3.3. Error prediction

The way to predict the output y at $(t+\tau)$ is based on the expansion in Taylor series. An approximation of the reference signal is done in the same way.

$$\hat{y}(t+\tau) = \sum_{k=0}^{\rho} y^{(k)}(t)\frac{\tau^k}{k!} + R(\tau^\rho) \tag{13}$$

The predicted output is rewritten in matrix form:

$$\hat{y}(t+\tau) \cong \begin{bmatrix} 1 & \tau & \frac{\tau^2}{2!} & \cdots & \frac{\tau^\rho}{\rho!} \end{bmatrix} \begin{bmatrix} y(t) \\ \dot{y}(t) \\ \vdots \\ y^{(\rho-1)}(t) \\ y^{(\rho)}(t) \end{bmatrix} \tag{14}$$

When the output $y(t)$ and these derivatives up to order τ. Then we can deduce the predicted output at $t+\tau$:

$$\hat{y}(t+\tau) \cong \begin{bmatrix} 1 & \tau & \frac{\tau^2}{2!} & \cdots & \frac{\tau^\rho}{\rho!} \end{bmatrix} L_y \tag{15}$$

with

$$L_y = \begin{bmatrix} h(x(t)) \\ L_f h(x(t)) \\ \vdots \\ L_f^{\rho-1} h(x(t)) \\ L_f^{\rho} h(x(t)) + L_g L_f^{\rho-1} h(x(t)) u(t) \end{bmatrix} \tag{16}$$

Similarly, we can deduce the expression of $\hat{w}$ at $t+\tau$ if we assume that the reference trajectory is known. The reference vector can be written as following:

$$\hat{w}(t+\tau) \cong \begin{bmatrix} 1 & \tau & \frac{\tau^2}{2!} & \cdots & \frac{\tau^\rho}{\rho!} \end{bmatrix} \begin{bmatrix} w(t) \\ \dot{w}(t) \\ \vdots \\ w^{(\rho-1)}(t) \\ w^{(\rho)}(t) \end{bmatrix} \tag{17}$$

So, we can define the predicted error at $(t+\tau)$ as:

$$\hat{e}_i(t+\tau) = \hat{y}_i(t+\tau) - \hat{w}_i(t+\tau) \tag{18}$$

With $1 \le i \le m$ and $\hat{e}_i$ the predicted error of ith output of the our system.

In the next paragraph, we take the quadratic criterion in its matrix form for the development of the control law.

3.4. Synthesis control law

The criterion that we consider here is the sum of all quadratic criteria built on each outputs of the system. We can rewriting the criterion function J_i by defining (7) in the matrix form:

$$\frac{\partial J_i}{\partial u} = 0_{p\times 1} \tag{19}$$

We denote:

$$E_i(t) = \begin{bmatrix} e_i(t) \\ \dot{e}_i(t) \\ \vdots \\ e^{(\rho_i-1)}(t) \\ e^{(\rho_i)}(t) \end{bmatrix} \quad and \quad \Lambda_i(\tau) = \begin{bmatrix} 1 \\ \tau \\ \vdots \\ \frac{\tau^{\rho_i-1}}{\rho_i-1!} \\ \frac{\tau^{\rho_i}}{\rho_i!} \end{bmatrix}^t \tag{20}$$

and the prediction error can be written

$$\hat{e}_i(t+\tau) = \Lambda_i(\tau)E_i(t) \tag{21}$$

To minimize the function cost (8) we can write:

$$J_i(t) = \frac{1}{2}\int_0^{T_i} E_i^t(t)\Lambda_i^t(\tau)\Lambda_i(\tau)E_i(t)d\tau \tag{22}$$

Since the vector E_i does not depend on τ but on t,

$$J_i(t) = \frac{1}{2}E_i^t(t)\int_0^{T_i} \Lambda_i^t(\tau,\rho_i)\Lambda_i(\tau,\rho_i)d\tau E_i(t) \tag{23}$$

For practical reasons, we denote the matrix $\Pi_i(T_i,\rho_i)$ of dimension $(\rho_i+1)\times(\rho_i+1)$, therefore we define the prediction matrix as follow:

$$\Pi_i(T_i,\rho_i) = \int_0^{T_i} \Lambda_i^t(\tau,\rho_i)\Lambda_i(\tau,\rho_i)d\tau \tag{24}$$

Then the criterion function J_i can written as:

$$J_i(t) = \frac{1}{2}E_i^t(t)\Pi_i(T_i,\rho_i)E_i(t) \tag{25}$$

Finally the global criterion function J are deduced in its matrix form:

$$\frac{\partial J}{\partial u} = \frac{1}{2}\sum_{i=1}^{m}\frac{\partial\left[E_i^t(t)\Pi_i(T_i,\rho_i)E_i(t)\right]}{\partial u} = 0_{p\times 1} \tag{26}$$

and deduce that,

$$\frac{\partial J}{\partial u} = \frac{1}{2}\sum_{i=1}^{m}\left(\frac{\partial E_i(t)}{\partial u}\right)^t \Pi_i(T_i,\rho_i)E_i(t) = 0_{p\times 1} \tag{27}$$

from (15),(17),(18),(20), E_i can be written as follow

$$E_i(t) = \begin{bmatrix} h_i(x(t)) - w_i(t) \\ L_f h_i(x(t)) - \dot{w}_i(t) \\ \vdots \\ L_f^{(\rho_i-1)}h_i(x(t)) - w_i^{(\rho_i-1)}(t) \\ L_f^{(\rho_i)}h_i(x(t)) - w_i^{(\rho_i)}(t) + L_g L_f^{(\rho_i-1)}h_i\ u \end{bmatrix} \tag{28}$$

to show up the control law expression,

$$E_i(t) = E_{p_i} + \begin{bmatrix} 0 \\ \vdots \\ 0 \\ \begin{bmatrix} L_{g_1}L_f^{(\rho_i-1)}h_i & \cdots & L_{g_p}L_f^{(\rho_i-1)}h_i \end{bmatrix}\begin{bmatrix} u_1 \\ \vdots \\ u_p \end{bmatrix} \end{bmatrix} \tag{29}$$

with

$$E_{p_i} = \begin{bmatrix} h_i(x(t)) - w_i(t) \\ L_f h_i(x(t)) - \dot{w}_i(t) \\ \vdots \\ L_f^{(\rho_i-1)}h_i(x(t)) - w_i^{(\rho_i-1)}(t) \\ L_f^{(\rho_i)}h_i(x(t)) - w_i^{(\rho_i)}(t) \end{bmatrix} \tag{30}$$

Therefore,

$$\left(\frac{\partial E_i(t)}{\partial u}\right)^t = \begin{bmatrix} L_{g_1}L_f^{(\rho_i-1)}h_i \\ \vdots \\ L_{g_p}L_f^{(\rho_i-1)}h_i \end{bmatrix}_{(p\times 1)} \tag{31}$$

and hence

$$\sum_{i=1}^{m}\begin{bmatrix} L_{g_1}L_f^{(\rho_i-1)}h_i \\ \vdots \\ L_{g_p}L_f^{(\rho_i-1)}h_i \end{bmatrix}_{(p\times 1)} \Pi_i^s(T_i,\rho_i)E_i(t) = 0_{p\times 1} \tag{32}$$

with Π_i^s is the last line of Π_i matrix. After development (more details in APPENDIX A), the matrix form of (32) can be deduced,

$$\begin{bmatrix} L_{g_1}L_f^{(\rho_1-1)}h_1 & \cdots & L_{g_1}L_f^{(\rho_m-1)}h_m \\ \vdots & \ddots & \vdots \\ L_{g_p}L_f^{(\rho_1-1)}h_1 & \cdots & L_{g_p}L_f^{(\rho_m-1)}h_m \end{bmatrix}\begin{bmatrix} \Pi_1^s E_1 \\ \vdots \\ \Pi_m^s E_m \end{bmatrix} = 0_{p\times 1} \tag{33}$$

$D(x)$ is non-singular matrix in $x = x^0$ (12), we can deduce that:

$$\begin{bmatrix} \Pi_1^s E_1 \\ \vdots \\ \Pi_m^s E_m \end{bmatrix}_{(m\times 1)} = 0_{m\times 1} \tag{34}$$

To deduce the control law analytic expression, the equation (34) can be separating into two part (more details in APPENDIX A) as following

$$\Pi^{ss}\ D(x) \begin{bmatrix} u_1 \\ \vdots \\ u_p \end{bmatrix} = -\ \Pi^{s} \begin{bmatrix} h_1 - w_1 \\ \vdots \\ L_f^{\rho_1} h_1 - w_1^{(\rho_1)} \\ \vdots \\ h_m - w_m \\ \vdots \\ L_f^{\rho_m} h_m - w_m^{(\rho_m)} \end{bmatrix} \tag{35}$$

we denote,

$$\Pi^{ss} = \begin{bmatrix} \Pi_1^{ss} & & 0 \\ & \ddots & \\ 0 & & \Pi_m^{ss} \end{bmatrix} \tag{36}$$

where Π_i^{ss} corresponds to the last element of vector Π_i^{s}, and

$$\Pi^{s} = \begin{bmatrix} \Pi_1^{s} & & 0 \\ & \ddots & \\ 0 & & \Pi_m^{s} \end{bmatrix} \tag{37}$$

To determine the control law u, we must calculate the inverse of the matrix $D^t(x)D(x)$. For this we assume that $\det(D^t(x)D(x))$ is non-singular matrix.

Finally, the analytical expression of the control law u can be written as follows:

$$u = -\left(D^t(x)D(x)\right)^{-1} D^t(x)\ K\ E_p \tag{38}$$

with $D(x)$ decoupling matrix. The gain matrix K and prediction error matrix E_p have the following form:

$$K = \begin{bmatrix} \Pi_1^{ss} & & 0 \\ & \ddots & \\ 0 & & \Pi_m^{ss} \end{bmatrix}^{-1} \begin{bmatrix} \Pi_1^{s} & & 0 \\ & \ddots & \\ 0 & & \Pi_m^{s} \end{bmatrix} \tag{39}$$

$$E_p = \begin{bmatrix} h_1 - w_1 \\ \vdots \\ L_f^{\rho_1} h_1 - w_1^{(\rho_1)} \\ \vdots \\ h_m - w_m \\ \vdots \\ L_f^{\rho_m} h_m - w_m^{(\rho_m)} \end{bmatrix} \tag{40}$$

Remarque 1. The analytical expression of the control law u given by 38 is available not only to the nonlinear SISO system as presented in [27] but also to MIMO system.

After the development of the control law, one must be asked the question of the closed loop system's stability. In this paper, the analysis of the closed loop system's stability is not detailed. To understand this issue, more information can be found in the work of [28] [29] and [30]. From these studies can be concluded that in the case of NCGPC, the stability of the closed loop system is guaranteed with the relative degree of each output is less than or equal to four, which is the case in the studied system.

4. SYNTHESIS CONTROL APPLIED TO A PATH FOLLOWING PROBLEM

In the section 2, a non-linear model in the horizontal plane is developed. The output and the input of the system are y and u respectively and the reference signal w of the reference path are known in advance.

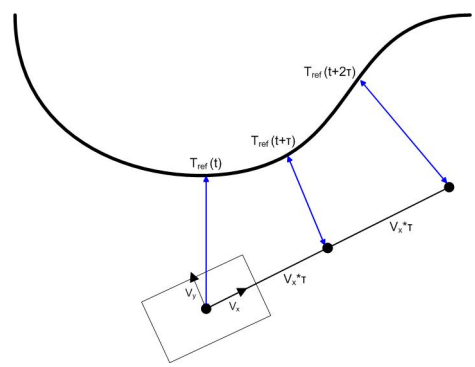

Fig 3: Scheme of predictive reference trajectory.

The output of our system is defined as follow::

$$y(t) = \begin{pmatrix} h_1 \\ h_2 \\ h_3 \end{pmatrix} \begin{pmatrix} \psi \\ X \\ Y \end{pmatrix}$$

and the input of the system u by:

$$u = \begin{pmatrix} u_1 \\ u_2 \end{pmatrix} = \begin{pmatrix} \beta_f \\ \beta_r \end{pmatrix}$$

and the reference signal or trajectory w by:

$$w = \begin{pmatrix} w_1 \\ w_2 \\ w_3 \end{pmatrix} = \begin{pmatrix} \psi_{ref} \\ X_{ref} \\ Y_{ref} \end{pmatrix}$$

We keep the same notation that is already used. It begins with the functions h_i.

$$\begin{cases} h_1 = \psi \\ h_2 = X \\ h_3 = Y \end{cases} \tag{41}$$

To synthesize the control law, we must calculate the vector relative degree ρ.

$$\begin{cases} L_f h_1 = V_\psi \\ L_f h_2 = V_x \cos\psi - V_y \sin\psi \\ L_f h_3 = V_x \sin\psi + V_y \cos\psi \end{cases} \tag{42}$$

We can deduce that $\rho_i > 1$ because for all $i = 1,2,3$, $L_g h_i = 0$. Then we apply a second time Lie derivative.

$$\begin{cases} L_f^2 h_1 = \frac{\partial L_f h_1}{\partial V_\psi} f_2 \\ L_f^2 h_2 = \frac{\partial L_f h_2}{\partial V_y} f_1 + \frac{\partial L_f h_2}{\partial \psi} f_3 \\ L_f^2 h_3 = \frac{\partial L_f h_3}{\partial V_y} f_1 + \frac{\partial L_f h_3}{\partial \psi} f_3 \end{cases} \tag{43}$$

$$\begin{cases} L_f^2 h_1 = a_{21} V_y + a_{22} V_\psi \\ L_f^2 h_2 = -\sin\psi \zeta_h - V_y V_\psi \cos\psi \\ L_f^2 h_3 = \cos\psi \zeta_h - V_y V_\psi \sin\psi \end{cases} \tag{44}$$

with

$$\zeta_h = \left(V_x V_\psi + a_{11} V_y + a_{12} V_\psi\right)$$

The different expressions of $L_{g_j} L_f h_i$ are non null for all $i = 1,2,3$ and $j = 1,2$. Hence we can deduce that all terms of the relative degree vector ρ are equal to $2 : \rho = \begin{pmatrix} \rho_1 & \rho_2 \end{pmatrix} = \begin{pmatrix} 2 & 2 \end{pmatrix}$.

$$\begin{cases} L_{g_1} L_f h_1 = b_{21} \\ L_{g_1} L_f h_2 = -b_{11} \sin\psi \\ L_{g_1} L_f h_3 = b_{11} \cos\psi \end{cases} \tag{45}$$

and

$$\begin{cases} L_{g_2} L_f h_1 = b_{22} \\ L_{g_2} L_f h_2 = -b_{12} \sin\psi \\ L_{g_2} L_f h_3 = b_{12} \cos\psi \end{cases} \tag{46}$$

and we deduce the decoupling matrix $D(x)$:

$$D(x) = \begin{bmatrix} b_{21} & b_{22} \\ -b_{11} \sin\psi & -b_{12} \sin\psi \\ b_{11} \cos\psi & b_{12} \cos\psi \end{bmatrix} \tag{47}$$

It's verified that the matrix $(D^t(x) D(x))$ is invertible.

Calculating the prediction error matrix:

$$E_p = \begin{bmatrix} h_1 - w_1 \\ L_f h_1 - \dot{w}_1 \\ L_f^2 h_1 - \ddot{w}_1 \\ h_2 - w_2 \\ L_f h_2 - \dot{w}_2 \\ L_f^2 h_2 - \ddot{w}_2 \\ h_3 - w_3 \\ L_f h_3 - \dot{w}_3 \\ L_f^2 h_3 - \ddot{w}_3 \end{bmatrix} = \begin{bmatrix} \psi - w_1 \\ V_\psi - \dot{w}_1 \\ a_{21} V_y + a_{22} V_\psi - \ddot{w}_1 \\ X - w_2 \\ V_x \cos\psi - V_y \sin\psi - \dot{w}_2 \\ -\zeta_h \sin\psi - V_y V_\psi \cos\psi - \ddot{w}_2 \\ Y - w_3 \\ V_x \sin\psi + V_y \cos\psi - \dot{w}_3 \\ \zeta_h \cos\psi - V_y V_\psi \sin\psi - \ddot{w}_3 \end{bmatrix} \tag{48}$$

Calculating the gain matrix K_i for e_i prediction error, then we deduce the gain matrix K defined in (50).

$$K_i = \begin{bmatrix} \frac{10}{3T_s^2} & \frac{10}{4T_s} & 1 \end{bmatrix} \tag{49}$$

$$K = \begin{bmatrix} K_1 & 0 & 0 \\ 0 & K_2 & 0 \\ 0 & 0 & K_3 \end{bmatrix} \tag{50}$$

Finally the control input can be computed by (38).

5. RESULTS AND DISCUSSION

The validation of the controller detailed in this paper has been achieved on a the mobile robot depicted on the figure 4. Manufactured by the Robosoft company, this platform, called SPIDO figure shown on figure (4), is electrically actuated, with two steering axles β_F and β_R, and four independent driving wheels. It is designed to move off-road with a speed up to 10m/s. It weights m is equal to $530kg$ and the two half wheel base used in the control law expression are $a = 0.67m$ and $b = 1.1m$. The last parameter attached to the robot design and required for the control is the vertical inertia I_z, which is approximated to $300kg.m^2$. In this application, the rear axle is not considered and set to zero, while the velocity control is not activated. As a result, the speed is regulated to a constant during each of the path tracking tests.

Fig 4: Experimental platform.

In order to proceed the motion control, the reference trajectory as well as the robot position and orientation has to be known. The experimental platform is the all-terrain four-wheel steering vehicle depicted on is shown in Figure(4). The vehicle weight is $420kg$ and the front and rear half wheel base are respectively $0.62m$ and $0.58m$. It is equipped with a Real Time Kinematic GPS (RTK-GPS). This sensor supplies a localization with respect to a reference station with the accuracy to within $\pm 2cm$.

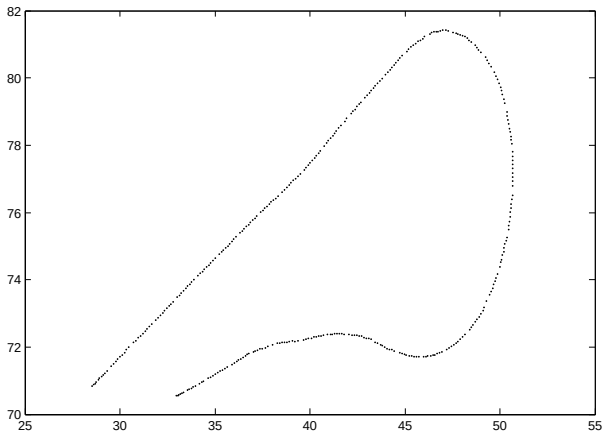

Fig 5: The reference trajectory.

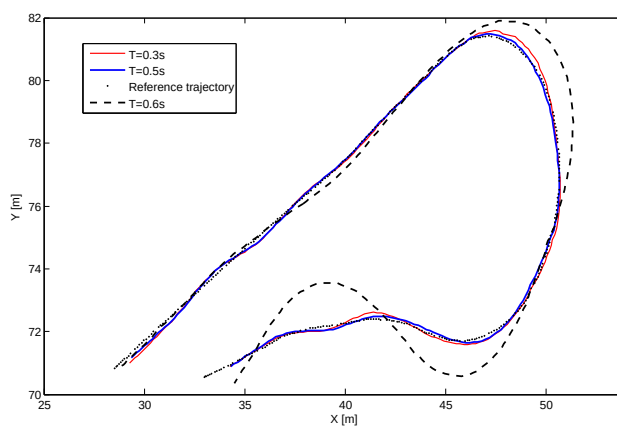

Fig 6: Trajectories at different prediction horizon time $T = 0.5s$, $T = 0.3s$ and $T = 0.6s$

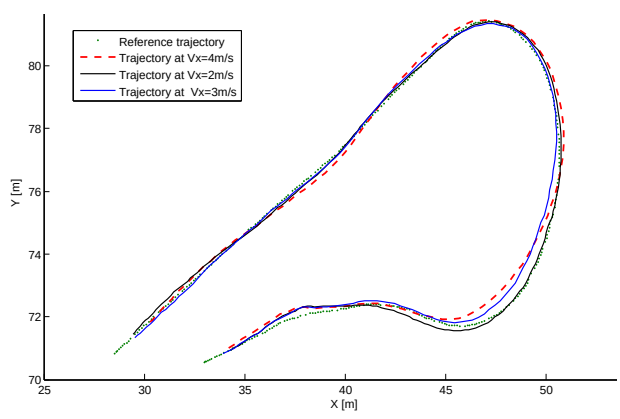

Fig 7: Comparison of trajectories at different velocities

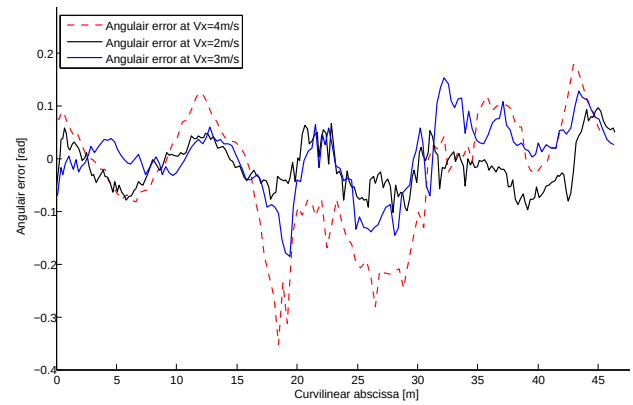

Fig 8: Angular deviation prediction horizon time $T = 0.5s$ [rad]

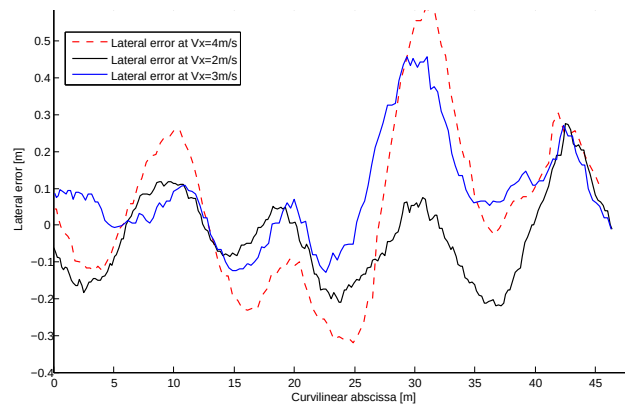

Fig 9: Lateral deviation prediction horizon time $T = 0.5s$ [m]

If control law (38) has implemented on the experimental platform, the matrix $(D^t(x)D(x))^{-1}$ and K can be calculated off-line to lighten the real time calculation. We must find the closest three points in the reference trajectory to the vehicle predicted position (Fig.3). Then we can deduce the reference signal $w = (w_1, w_2, w_3)$ to calculated the prediction error matrix E. In our case, the ground was wet grass irregular pattern, where the slip phenomena cannot be neglected. The path to be followed is recorded by a preliminary run achieved in manual driving. The classical O paths (Fig.5) was used for testing the controller at different velocities, it is plotted on (Fig.7). The lateral and angular error during the automatic following of the reference trajectory has been recorded at different velocity (Fig.9) and (Fig.8).

At the same conditions (reference path, velocity and the type of the ground), we observe in Fig.6 a difference when we compare the path trajectory at different prediction horizon times $T = 0.5s$ and $T = 0.6s$. The following path tracking is better at prediction horizon time $T = 0.5s$ than $T = 0.3s$ and $T = 0.6s$. The

gain matrix K defined by eq.(39)is inversely proportional to the prediction horizon T. So, the using for $T = 0.6s$ decrease the gain K. In the other way, when the prediction horizon decreases by using $T = 0.3s$, the prediction distance (in our case $T * Vx * 3$ Fig.3) decreases too. So, We can not increase or decrease the prediction horizon time infinitely. In our case, the prediction horizon T is chosen experimentally. We will try in future work, to find an optimal prediction horizon. Therefore, we can deduce that the prediction horizon depend on the dynamic of the system and not only of the velocity V_x of the robot.

We must notice that our controller model is based on constant front and rear cornering stiffnesses. This is not completely true when there is front/rear load transfer or changes of ground materials. But thanks to controller robustness, the control law ensure a trajectory tracking with low tracking error. The results obtained are comparable to those present in [31] in which the cornering stiffnesses is estimated on line. The presence and the variation of sliding phenomena at high speed influence certainly the path following but the choice of robust controller can be able to stabilize the system and resolve this problems.

The tracking error during following the path was recorded and reported on (Fig.8) and (Fig.9). We compare the lateral and angular error at different velocities ($2m/s$, $3m/s$ and $4m/s$) in (Fig.8) and (Fig.9) respectively. This results shows clearly the dependency of the non-linear control law to the velocity of the vehicle and we can deduce the maximum speed for this path. In the validation task, the maximum velocity of the experimental vehicle is $4m.s^{-1}$. Nevertheless, even at this speed, when the robot has to track paths with small radii of curvature on slippery ground surface, then the relevance of the proposed approach is demonstrated. Significant improvements in robot behavior and in path tracking accuracy can be recorded ($V_x = 4m/s$ deduced from the relation $MkV_x^2 < \mu Mg$, where g: gravity, M: vehicle mass and μ is a constant).

It can be observed that the lateral error is more important then the angular error when we compare (Fig.8) and (Fig.9). If we look closely the function cost (8) and the error expression (6) we can deduce that there is no weighting between the different output of the system. In our case the lateral deviation is more important then the angular deviation. So, the introduction of weighting in the function cost to give preferential treatment to the lateral error can reduce it .

6. CONCLUSIONS

In this paper, a non-linear predictive controller that ensures path tracking task for fast off-road robot is proposed, validated and discussed. The control strategy based kinematics models and neglected the vehicle dynamic is enable to stabilize the robot on the reference trajectory because the sliding phenomena is very important and can not be neglected in our case. This phenomena has been explicitly taken into account by combining the kinematics and dynamics model of the vehicle. The controller is based on a dynamic model of the vehicle which considers lateral wheel slippage. The latter could be significant and are unavoidable particularly when moving fast and cornering and when the ground surface is slippery.

This controller supply an analytical expression of the control input u that reduces the real time calculation which simplifies the implementation of the controller algorithm. The study proposed in this paper opens the way to integrated a variable prediction horizon and estimate the front and rear cornering stiffnesses C_f and C_r that will be calculated on-line. In the other way, the prediction controller can be improved by introducing weighting on the error in the function cost.

REFERENCES

[1] C. Samson. Control of chained systems application to path following and time-varying point-stabilization of mobile robots. Automatic Control, IEEE Transactions on, 40(1):64 –77, jan 1995.

[2] G. Campion, G. Bastin, and B. d' Andréa-Novel. Structural properties and classification of kinematic and dynamic models of wheeled mobile robots. In Ieee international conference on robotics and automation, pages 462–469, Atlanta, Georgia (USA), 1993.

[3] T. Peynot and S. Lacroix. Enhanced locomotion control for a planetary rover. In Intelligent Robots and Systems, 2003. (IROS 2003). Proceedings. 2003 IEEE/RSJ International Conference on, volume 1, pages 311 – 316 vol.1, oct. 2003.

[4] M. Nitulescu. Mobile robot tracking control experiments along memorized planed trajectories. In Automation, Quality and Testing, Robotics, 2006 IEEE International Conference on, volume 2, pages 296 –301, may 2006.

[5] E. Lucet, C. Grand, D. Salle, and P. Bidaud. Dynamic yaw and velocity control of the 6wd skid-steering mobile robot roburoc6 using sliding mode technique. In Intelligent Robots and Systems, 2009. IROS 2009. IEEE/RSJ International Conference on, pages 4220 –4225, oct. 2009.

[6] R. Eaton, H. Pota, and J. Katupitiya. Path tracking control of agricultural tractors with

compensation for steering dynamics. In Decision and Control, 2009 held jointly with the 2009 28th Chinese Control Conference. CDC/CCC 2009. Proceedings of the 48th IEEE Conference on, pages 7357 –7362, dec. 2009.

[7] B. d' Andréa-Novel, G. Campion, and G. Bastin. Control of wheeled mobile robots not satisfying ideal velocity constraints: a singular perturbation approach. International Journal of Robust and Nonlinear Control, 5(4):243–267, 1995.

[8] Zhaoheng and Liu. Characterisation of optimal human driver model and stability of a tractor-semitrailer vehicle system with time delay. Mechanical Systems and Signal Processing, 21(5):2080 – 2098, 2007.

[9] R. Lenain, B. Thuilot, C. Cariou, and P. Martinet. Mobile robot control in presence of sliding: Application to agricultural vehicle path tracking. In Decision and Control, 2006 45th IEEE Conference on, pages 6004 –6009, dec. 2006.

[10] D. Wang and C.B. Low. An analysis of wheeled mobile robots in the presence of skidding and slipping: Control design perspective. In IEEE International Conference on Robotics and Automation (ICRA), pages 2379–2384, Roma, Italy, 2007.

[11] R. Lenain, B. Thuilot, O. Hach, and P. Martinet. High-speed mobile robot control in off-road conditions: a multi-model based adaptive approach. In EEE International Conference on Robotics and Automation, ICRA'11, page 6143:6149, 2011.

[12] L. Zadeh and B. Whalen. On optimal control and linear programming. Automatic Control, IRE Transactions on, 7(4):45 – 46, jul 1962.

[13] J. Richalet, A. Rault, J.L. Testud, and J. Papon. Model predictive heuristic control: Applications to industrial processes. Automatica, 14(5):413 – 428, 1978.

[14] A. Chemori and N. Marchand. A prediction-based nonlinear controller for stabilization of a non-minimum phase pvtol aircraft. International Journal of Robust and Nonlinear Control, 18(8):876–889, 2008.

[15] V.M. Zavala, C.D. Laird, and L.T. Biegler. Fast implementations and rigorous models: Can both be accommodated in nmpc? International Journal of Robust and Nonlinear Control, 18(8):800–815, 2008.

[16] G. Klanar and I. Łkrjanc. Tracking-error model-based predictive control for mobile robots in real time. Robotics and Autonomous Systems, 55(6):460 – 469, 2007.

[17] J. E. Normey-Rico, J. Gomez-Ortega, and E. F. Camacho. A smith-predictor-based generalised predictive controller for mobile robot path-tracking. Control Engineering Practice, 7(6):729 – 740, 1999.

[18] T.D. Gillespie. Fundamentals of vehicle dynamics. SAE International, Warrendale, U.S.A., 1992.

[19] C.C. DeWit and P. Lischinsky. Adaptive friction compensation with partially known dynamic friction model. International Journal of Adaptive Control and Signal Processing, 11(1):65–80, 1997.

[20] P. R. Dahl. Solid friction damping of mechanical vibrations. AIAA Journal, 14(12):1675–1682, 1976.

[21] H.B. Pacejka and al. Magic formula tyre model with transient properties. Vehicle System Dynamics, 27:234–249, 1997.

[22] N. Bouton. Stabilité dynamique des véhicule légers tout terrain. Vision er robotique, Université Blaise Pascal Clermont II, Novembre 2009.

[23] J. Ackermann and W. Sienel. Robust yaw damping of cars with front and rear wheel steering. Control Systems Technology, IEEE Transactions on, 1(1):15 –20, mar 1993.

[24] R. Anderson and D.M. Bevly. Estimation of tire cornering stiffness using gps to improve model based estimation of vehicle states. In Intelligent Vehicles Symposium, 2005. Proceedings. IEEE, pages 801 – 806, june 2005.

[25] C. Sentouh, S. Mammar, and S. Glaser. Simultaneous vehicle state and road attributes estimation using unknown input proportional-integral observer. In Intelligent Vehicles Symposium, 2008 IEEE, pages 690 –696, june 2008.

[26] M. Krid and F. Ben Amar. A dynamic based path tracking controller for a fast rover with independent steering and drive. In International Conference on Climbing and Walking Robots and the Support Technologies for Mobile Machines, Septembre 2011.

[27] M. Dabo, H. Chafouk, and N. Langlois. Unconstrained ncgpc with a guaranteed closed-loop stability: Case of nonlinear siso systems with the relative degree greater than four. In Decision and Control, 2009 held jointly with the 2009 28th Chinese Control Conference. CDC/CCC 2009. Proceedings of the 48th IEEE Conference on, pages 1980 –1985, dec. 2009.

[28] W.H. Chen. Predictive control of general nonlinear systems using approximation. Control Theory and Applications, IEE Proceedings -, 151(2):137 – 144, march 2004.

[29] P. J. Gawthrop, D.J. Ballance, and W.H. Chen. Optimal control of nonlinear systems: a predictive control approach. Automatica, 39(4):633–

641, April 2003. Final version as accepted by Automatica supplied by the author.

[30] M. Dabo. Commande prédictive généralisée non linéaire à temps continu des systèmes complexes. Automatique et traitement du signal, Université de Rouen, MAI 2010.

[31] R. Lenain, B. Thuilot, C. Cariou, and P. Martiner. Mixed kinematic and dynamic sideslip angle observer for accurate control of fast off road mobile robots. Journal of Filed Robotics, 2010, vol. 27, nř 2, p. 181-196, 27:181–196, 2010.

APPENDIX A

$$\begin{bmatrix} L_{g_1}L_f^{(\rho_1-1)}h_1 \\ \vdots \\ L_{g_p}L_f^{(\rho_1-1)}h_1 \end{bmatrix} \Pi_1^s(T_1,\rho_1)E_1(t) + \cdots + \begin{bmatrix} L_{g_1}L_f^{(\rho_m-1)}h_m \\ \vdots \\ L_{g_p}L_f^{(\rho_m-1)}h_m \end{bmatrix} \Pi_m^s(T_m,\rho_m)E_m(t) = 0_{p\times 1} \tag{A,1}$$

$$\begin{bmatrix} \Pi_1^s E_1 \\ \vdots \\ \Pi_m^s E_m \end{bmatrix}_{(m\times 1)} = \begin{bmatrix} \Pi_1^s & & 0 \\ & \ddots & \\ 0 & & \Pi_m^s \end{bmatrix} \begin{bmatrix} \begin{matrix} h_1 - w_1 \\ L_f h_1 - \dot{w}_1 \\ \vdots \\ L_f^{\rho_1-1}h_1 - w_1^{(\rho_1-1)} \\ L_f^{\rho_1}h_1 - w_1^{(\rho_1)} \\ \vdots \\ h_m - w_m \\ L_f h_m - \dot{w}_m \\ \vdots \\ L_f^{\rho_1-1}h_m - w_m^{(\rho_m-1)} \\ L_f^{\rho_m}h_m - w_m^{(\rho_m)} \end{matrix} & \begin{matrix} + \\ \\ \\ \\ \\ \vdots \\ \\ \\ \\ + \\ \\ \\ \end{matrix} & \begin{matrix} 0 \\ \vdots \\ \begin{bmatrix} L_{g_1}L_f^{(\rho_i-1)}h_1 & \cdots & L_{g_p}L_f^{(\rho_i-1)}h_1 \end{bmatrix} \begin{bmatrix} u_1 \\ \vdots \\ u_p \end{bmatrix} \\ \\ \\ \vdots \\ 0 \\ \vdots \\ \begin{bmatrix} L_{g_1}L_f^{(\rho_i-1)}h_m & \cdots & L_{g_p}L_f^{(\rho_i-1)}h_m \end{bmatrix} \begin{bmatrix} u_1 \\ \vdots \\ u_p \end{bmatrix} \end{matrix} \end{bmatrix} \tag{A,2}$$

$$\begin{bmatrix} \Pi_1^{ss} & & 0 \\ & \ddots & \\ 0 & & \Pi_m^{ss} \end{bmatrix} \begin{bmatrix} L_{g_1}L_f^{(\rho_1-1)}h_1 & \cdots & L_{g_p}L_f^{(\rho_1-1)}h_1 \\ \vdots & \ddots & \vdots \\ L_{g_1}L_f^{(\rho_m-1)}h_m & \cdots & L_{g_p}L_f^{(\rho_m-1)}h_m \end{bmatrix} \begin{bmatrix} u_1 \\ \vdots \\ u_p \end{bmatrix} = - \begin{bmatrix} \Pi_1^s & & 0 \\ & \ddots & \\ 0 & & \Pi_m^s \end{bmatrix} \begin{bmatrix} h_1 - w_1 \\ \vdots \\ L_f^{\rho_1}h_1 - w_1^{(\rho_1)} \\ \vdots \\ h_m - w_m \\ \vdots \\ L_f^{\rho_m}h_m - w_m^{(\rho_m)} \end{bmatrix} \tag{A,3}$$

$$\begin{bmatrix} u_1 \\ \vdots \\ u_p \end{bmatrix} = -\left(D^t(x)D(x)\right)^{-1} D^t(x) \begin{bmatrix} K_1 & & 0 \\ & \ddots & \\ 0 & & K_m \end{bmatrix}_{\left[p\times \sum_{i=1}^{m}(\rho_i+1)\right]} \begin{bmatrix} h_1 - w_1 \\ \vdots \\ L_f^{\rho_1}h_1 - w_1^{(\rho_1)} \\ \vdots \\ h_m - w_m \\ \vdots \\ L_f^{\rho_m}h_m - w_m^{(\rho_m)} \end{bmatrix}_{\left[\sum_{i=1}^{m}(\rho_i+1)\times 1\right]} \tag{A,4}$$